

Study on Electrochemical Property of As-Cast and Annealed A_2B_7 Type La-Mg-Ni System Alloy

YANG Liying¹, DONG Xiaoping¹, YANG Liqing²,
LI Zhiyuan¹, GENG Xiaoguang¹

(1. College of Quality and Technical Supervision, Hebei University, Baoding, 071002, China)
(2. School of Information, Inner Mongolia University of Science and Technology, Baotou 014010, China)



杨丽颖

Abstract: In order to improve electrochemical property of as-cast La_3MgNi_{14} alloy, the alloy was annealed at 1 123, 1 223 and 1 323 K under 0.3 MPa Argon atmospheres for 10 h. Microstructures and electrochemical properties of different annealed alloys have been investigated by XRD, SEM and electrochemical experiment. The obtained results show that as-cast alloy and alloy annealed at 1 123 K are composed of $LaNi_5$, $(La, Mg)_2Ni_7$ and a small amount of $LaNi_2$ phases. There are some $LaNi_5$, $(La, Mg)_2Ni_7$ and $(La, Mg)Ni_3$ phases in alloy annealed at 1 223 K. However, $LaNi_5$ and $(La, Mg)Ni_3$ phases became main phase at 1 323 K. Compared by as-cast alloy, composition of annealed alloys is more homogeneous, and grains of annealed alloys are coarsened. With increasing annealing temperature, some electrochemical properties and kinetic parameters of the alloys, involving maximum discharge capacity, discharge efficiency, cyclic stability, high-rate discharge ability (HRD) of the alloys all increase, however, potential difference and charge-transfer reaction resistance of the alloys decrease. In order to balance between discharge capacity and cyclic stability, the most suitable annealing temperature for preparation of La_3MgNi_{14} alloy is recommended to be 1 323 K in present work.

Key words: annealing temperature; La-Mg-Ni system alloy; electrochemical property

CLC number: TG139.7 **Document code:** A **Article ID:** 1674-3962(2011)05-0046-05

铸态和退火态 A_2B_7 型 La-Mg-Ni 系合金的电化学研究

杨丽颖¹, 董小平¹, 杨丽清², 李志原¹, 耿晓光¹

(1. 河北大学质量技术监督学院, 河北 保定 071002)

(2. 内蒙古科技大学 信息学院, 内蒙古 包头 014010)

摘要: 为了改善铸态 La_3MgNi_{14} 合金的电化学性能, 在 0.3 MPa 氩气气氛下对 La_3MgNi_{14} 合金进行了 10 h 退火处理, 退火温度分别为 1 123, 1 223 和 1 323 K。采用 X 射线衍射 (XRD)、扫描电镜 (SEM) 和电化学实验研究了合金的微观结构和电化学性能。结果表明, 铸态及 1 123 K 温度退火后的合金由 $LaNi_5$ 相、 $(La, Mg)_2Ni_7$ 相以及少量的 $LaNi_2$ 相组成。1 223 K 温度退火后合金含有 $LaNi_5$, $(La, Mg)_2Ni_7$ 和 $(La, Mg)Ni_3$ 相。1 323 K 温度退火后合金的主相为 $LaNi_5$ 和 $(La, Mg)Ni_3$ 相。与铸态合金相比, 退火后合金组织更加均匀, 晶粒长大。随着退火温度的增加, 合金的一些电化学性能 (如最大放电容量、放电效率、循环稳定性) 以及动力学参数 (如高倍率放电性能) 增强, 而电位差和电荷迁移电阻降低。在本研究范围内, 为了放电容量和循环稳定性之间的平衡, 铸态 La_3MgNi_{14} 合金的适宜退火温度为 1 323 K。

关键词: 退火温度; La-Mg-Ni 系合金; 电化学性能

1 Introduction

As we known, clean hydrogen energy has sprung up due to

low or zero carbon energy. Hydrogen storage is more important to all hydrogen energy system. Storage of metal hydride is one of chemical methods of hydrogen storage. A series of metal hydride materials have been discovered, such as rare-earth based AB_3 -type alloy^[1], rare-earth Magnesium based A_2B_7 -type alloy^[2], AB_2 -type Laves phase alloy^[3], Mg-based alloy^[4], and V-based solid solution alloy^[5]. Of these alloys, rare-earth based AB_3 -type alloy has realized large-scale industrialization^[6]. However, commercial AB_3 -type hydrogen storage alloy could not meet demand of Ni/MH power battery applied to high-

Received date: 2010-09-09

Foundation Item: National 863 Program (2007AA03Z230); Natural Science Foundation of Hebei Province (E2010000301); Natural Science Research Planned Project of Hebei University (2009-152)

Biography: Yang Liying, Doctor, lecturer

er power HEV owing to its low discharge capacity (310 ~ 330 mA · h/g) [1]. Therefore, higher capacity of hydrogen storage alloy negative electrode is one of main approaches to improvement of energy density of Ni/MH battery. In a decade, La-Mg-Ni system A₂B₇-type alloys with higher discharge capacity were paid much attention as the candidates for negative electrode materials of Ni/MH power batteries owing to their higher discharge capacity (>350 mA · h/g) [7] compared to AB₅-type alloys. However, La-Mg-Ni system hydrogen storage alloy can not industrially product in their present state owing to fast discharge capacity degradation in the process of charge/discharge cycles. For slowing up capacity degradation of La-Mg-Ni system alloy electrodes, researchers have carried out lots of investigations and obtained significant results. It is well known that manufacture technology is extremely important for improving performances of the alloys. Kohno *et al.* [8] found that La₃MgNi₁₄-type electrode alloy La_{0.75}Mg_{0.25}Ni_{3.0}Co_{0.5} has capacity of 390 mA · h/g and capacity decay is slow during 30 charge/discharge cycles. Zhang *et al.* [9] investigated that annealing treatment is favorable for improvement of electrochemical property of La_{1.5}Mg_{0.5}Ni₇ alloy. Discharge capacities of as-cast and annealed at 1 173 K alloys are 358.2 and 402.5 mA · h/g, respectively. Cycling stability was improved obviously from 47% (as-cast) to 82% (at 1 173 K) after about 150 cycles. Pan *et al.* [10] prepared La_{0.67}Mg_{0.33}Ni_{2.5}Co_{0.5} alloy annealed at 1 123 K and 1 223 K. Electrochemical results show that, in three alloys (as-cast, 1 123, 1 223 K), discharge capacity of the alloy annealed at 1 123 K is higher, and cycling stability of the alloy annealed at 1 223 K is better, respectively. The above-mentioned results show that appropriate annealing temperature is effective way to improve discharge capacity and cyclic stability of hydrogen storage alloys. In this paper, in order to improve further cyclic stability of the La₃MgNi₁₄ alloy, effects of annealing treatment on electrochemical behaviors were investigated systemically.

2 Experimental

La₃MgNi₁₄ as-cast alloy was prepared using induction melting in high purity helium with 0.04 MPa. Some of as-cast alloys by sealed under vacuum atmosphere, and in quartz tube were annealed at 1 123, 1 223 and 1 323 K under 0.3 MPa Argon atmospheres for 10 h, respectively. Phase structure of alloys was determined by X-ray diffractometer of D_{MAX}-RB in Rigaku Ltd. Diffraction was performed with CuK_{α1} radiation filtered by graphite. Experimental parameters for determining phase structure are 150 mA, 40 kV and 8°/min, respectively. Samples thus prepared were etched with a 15 g FeCl₃ + 50 ml HCl + 100 ml deionized aqueous solution. Morphologies of the alloys were observed by SEM of Cambridge S-360.

Electrode pellets with 15 mm diameter were prepared by mixing 0.200 g alloy powder (≤74 μm) with Ni carbonyl powder in a mass ratio of 1:4 together, and then pressing under 35 MPa. Electrode pellets were immersed in 6 mol/L KOH solution containing 15 g/L LiOH for 24 h in order to fully wet the electrodes before measurement. Electrode pellet was fixed on terminal line of negative electrode of open tri-electrode cell. Ni (OH)₂/NiOOH is positive electrode of experimental cell, Hg/HgO is reference electrode and 6 mol/L KOH solution containing 15 g/L LiOH is electrolyte. Electrochemical performance of the alloy was measured by battery test system of Land-CT2001A. Voltage between negative electrode and reference electrode is defined as discharge voltage. Each electrode was discharged to cut-off potential -0.500 V vs. Hg/HgO reference electrode. Properties of the electrodes were measured with

current density of 100 mA/g. High-rate discharge abilities (HRDs) of the alloys were determined at a series of current densities. Electrochemical impedance spectroscopy (EIS) and potentiodynamic polarization curves were conducted at 50% depth of discharge (DOD) using PARSTAT 2273 advanced electrochemical system. Before measured, the electrodes were completely activated by charging/discharging cycles. EIS spectra of the electrodes were obtained in frequency range of 10 KHz to 5 MHz with amplitude of 5 mV under open-circuit condition. Environment temperature of measurement was kept at 303 K.

3 Results and discussion

3.1 Property of the electrode

Cycle behaviors of the as-cast and annealed La₃MgNi₁₄ alloys are shown in Fig. 1. As can be seen, maximum discharge capacities are 329.1 mA · h/g, 347.6 mA · h/g, 360.0 mA · h/g and 383.0 mA · h/g for as-cast alloy, the alloys annealed at 1 123 K, 1 223 K and 1 323 K, respectively. It is also ascertained from Fig. 1 that absolute value of slope of cyclic stability curves of the as-cast and annealed at 1 123, 1 223 and 1 323 K alloys is about 1.074, 0.859, 0.619 and 0.534, respectively, suggesting that annealing treatment can enhance cyclic stabilities of the alloys, that is to say, after 250 charging/discharging cycles, capacity retention rate of the alloys is 17.93%, 39.99%, 59.11%, 62.89% for as-cast alloy and annealed alloys at 1 123, 1 223, 1 323 K, respectively.

Charge and discharge potential curves of as-cast and annealed La₃MgNi₁₄ alloys at maximum discharge capacity are presented in Fig. 2. From Fig. 2, it can be obtained that discharge potentials of the alloys at 50% depth of discharge (DOD) increase with rising annealing temperature. Potentials of charge/discharge are 0.951 8/0.883 0, 0.944 6/0.897 8, 0.932 8/0.909 3, 0.926 8/0.909 9 V for as-cast alloy, the alloys annealed at 1 123, 1 223 and 1 323 K, respectively. Potential difference of 50% depth of charge (DOC) and 50% depth of discharge (DOD) decrease from 68.6 mV (as-cast) to 16.7 mV (annealing temperature at 1 323 K) with increasing annealing temperature. Discharge efficiency of the alloy electrode, which is denoted by ratio of discharge capacity to charge capacity, is related to potential difference and widths of discharge potential plateaus. The smaller the potential difference is, the wider the discharge potential plateau is, and the more the discharge efficiency is. From Fig. 2, it is also found that widths of discharge potential plateaus of the alloys are ranked in sequence 1 323 K > 1 223 K > 1 123 K > as-cast. Moreover, discharge efficiency of the alloys increase from 73.13% (as-cast) to 85.11% (annealing temperature at 1 323 K) with increasing annealing temperature. Therefore, the results further show that annealing temperature can enhance discharge capacities of the alloys in our experiment.

High rate discharge ability (HRD), which is determined mainly by electrochemical kinetic property of the alloy electrode, is examined and shown in Fig. 3. High rate discharge ability (HRD) is defined as following equation:

$$HRD = \frac{C_d}{C_{100}} \times 100\% \quad (1)$$

where C_d is discharge capacity at discharge current density I_d at cut-off potential of -0.500 V vs. Hg/HgO reference electrode, C_{100} is discharge capacity at discharge current density $I = 100$ mA/g also at cut-off potential of -0.500 V vs. Hg/HgO reference electrode. High-rate discharge ability (HRD) decrease with increasing discharge current density I_d . For example, for the annealed alloy at 1 323 K, high-

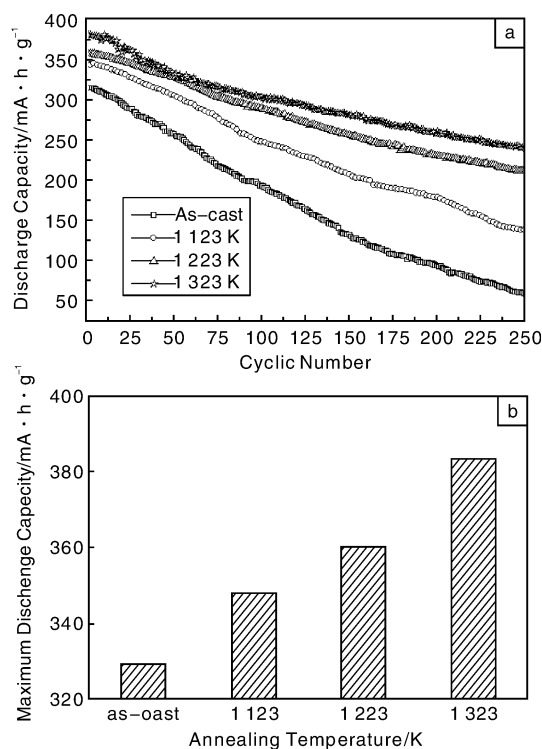


Fig. 1 Cycle behaviors of the as-cast and annealed $\text{La}_3\text{MgNi}_{14}$ alloys: discharge capacity (a) and maximum discharge capacity (b)

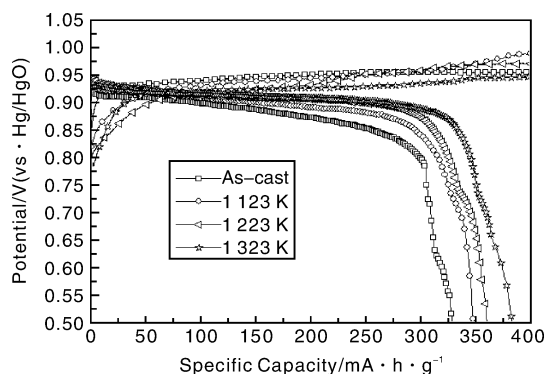
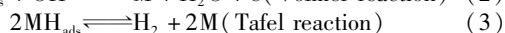
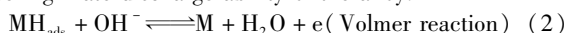


Fig. 2 Charge and discharge potential curves of as-cast and annealed $\text{La}_3\text{MgNi}_{14}$ alloys at maximum discharge capacity

rate discharge ability (HRD) of the alloy decrease from 94.50% ($I_d = 200 \text{ mA/g}$) to 62.50% ($I_d = 800 \text{ mA/g}$) with rising current density (Fig. 3). Owing to rising discharge current density, increasing hydrogen atoms diffused to surface of the alloy particles is too late to arise reaction of electron transfer (i.e. Volmer process), as shown in formula (2). Hydrogen gas directly desorbs, i.e. scale of the process of Tafel reaction increase (as shown in formula (3)). Consequently, mechanism of Volmer-Tafel leads to the decrease of discharge capacity of the alloy electrode, and decrease high-rate discharge ability of the alloy.



Gradient of curve of high-rate discharge ability reflects sensitivity of high-rate discharge ability and variation of discharge current density. From Fig. 3, it is also found that in

200 ~ 800 mA/g range, high-rate discharge ability of the alloys increase with increasing annealing temperature. Such as 500 mA/g, HRDs of the as-cast and annealed alloys enhance from 56.10% (as-cast) to 62.50% (at 1 323 K) with increasing annealing temperature.

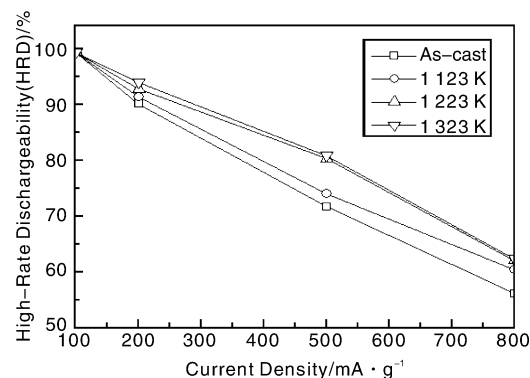


Fig. 3 High-rate discharge abilities (HRDs) of as-cast and annealed alloys

3.2 Discussion of property of the alloy electrode

XRD patterns of the as-cast and annealed $\text{La}_3\text{MgNi}_{14}$ alloys were exhibited in Fig. 4. As shown in Fig. 4, the as-cast and annealed (at 1 123 K) alloys are composed of LaNi_5 , $(\text{La}, \text{Mg})_2\text{Ni}_7$ and a small amount of LaNi_2 phases. Phase compositions of the alloys obviously change with rising annealing temperature. There are LaNi_5 , $(\text{La}, \text{Mg})_2\text{Ni}_7$ and $(\text{La}, \text{Mg})\text{Ni}_3$ phases in the annealed alloy at 1 223 K. However, LaNi_5 and $(\text{La}, \text{Mg})\text{Ni}_3$ phases became main phase at 1 323 K. With increasing annealing temperature, relative intensity of LaNi_5 phase peak increases because rising annealing temperature benefits formation of LaNi_5 phase according to La-Ni phase diagram^[11], suggesting that relative amount of LaNi_5 phase increase.

Microstructures of as-cast and annealed $\text{La}_3\text{MgNi}_{14}$ alloys were illustrated in Fig. 5. It should be noted from Fig. 5 that when annealing temperature increase, columnar texture decrease and massive texture increase in the annealed alloy at 1 223 K, massive texture is major in the annealed alloy at 1 323 K. In addition, for $\text{La}_3\text{MgNi}_{14}$ alloy, isothermal annealing is carried out at the same temperature, there is equal degree of supercooling during cooling. By contrast, composition of the annealed alloys is more homogeneous, grain boundaries are more definite, and grains of the alloys are coarsened.

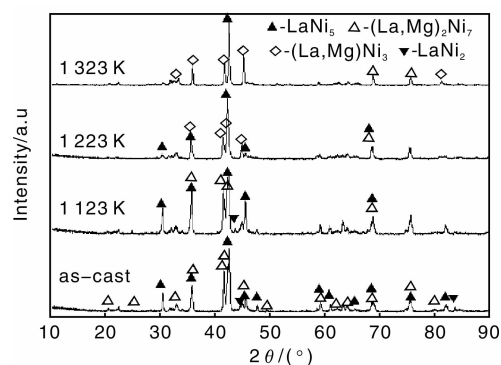


Fig. 4 XRD patterns of the as-cast and annealed $\text{La}_3\text{MgNi}_{14}$ alloys

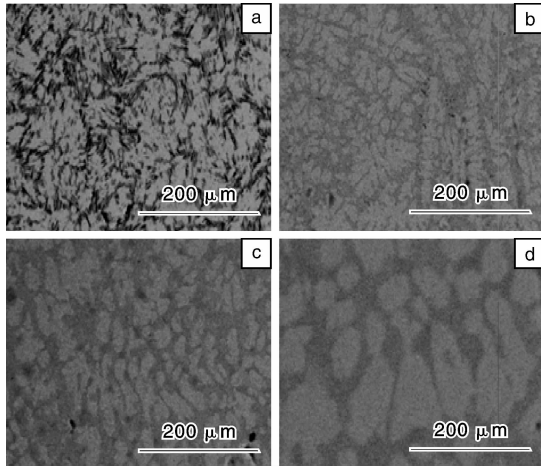


Fig. 5 Microstructure of as-cast and annealed La₃MgNi₁₄ alloys
(a) as-cast, (b) 1 123 K, (c) 1 223 K, and (d) 1 323 K

In our experiment, annealing treatment is helpful to enhancing maximum discharge capacity of the alloy, which monotonously increases with increasing annealing temperature. Result is related to phase component. At 1 223 K and 1 323 K, appearance of (La, Mg)Ni₃ phase and disappearance of LaNi₂ phase are favorable for improving discharge capacity. It can be derived from calculate model of Dunlap *et al.* [12] that ideal capacity of hydrogen storage (H/M) for La₂Ni₇ phase is 1.17, but that of LaNi₃ phase is 1.25 [13]. Therefore, the annealed alloys at 1 223 K and 1 323 K have higher discharge capacity. In addition, LaNi₅ phase is not only used as hydrogen absorption phase, but also as catalytic phase, and enhances utilization efficiency of hydrogen absorption for (La, Mg)Ni₃ or (La, Mg)₂Ni₇ phase. Therefore, with increasing annealing temperature, the increase of relative amount of LaNi₅ phase is favorable for improving kinetics of hydriding-dehydriding reaction of the alloys, and high-rate discharge ability (HRD) is improved. In addition, annealing treatment can decrease lattice strain and defects and improve the alloy's structure homogenization. These features weaken pulverization and strengthen anti-oxidation/corrosion capabilities during charge/discharge process in KOH/LiOH electrolyte. Owing to occurrence of electrochemical corrosion among grains in alkaline solution, resistance capability of corrosion of coarsened grains better than that of fined grains [14]. Therefore, annealing treatment can enhance cyclic life of the alloy in present work.

It has been reported that electrochemical impedance spectroscopy (EIS) is very useful to analyze kinetics of hydriding-dehydriding reaction of electrodes. Electrochemical impedance spectra of La₃MgNi₁₄ alloy electrodes at 50% DOD at 303 K were shown in Fig. 6. Proposed equivalent circuit for the alloy electrode was shown in Fig. 7. Contact resistance (R_f) and charge-transfer reaction resistance (R_{ct}) were obtained by fitting equivalent circuit in Table 1. For all the as-cast and annealed La₃MgNi₁₄ alloys, as shown in Fig. 6, at high and medium frequency, plot starts as capacitive loop, respectively, and, as the frequency further decreases, it changes to a straight line. According to result reported by Evgenij *et al.* [15–16], measured capacitive loop A in high-frequency region is ascribed to resistance and capacitance of current collector and pellet made of alloy powder. While me-

dium-frequency capacitive loop B is considered to be charge-transfer process at electrode/electrolyte interface, as shown in equation:

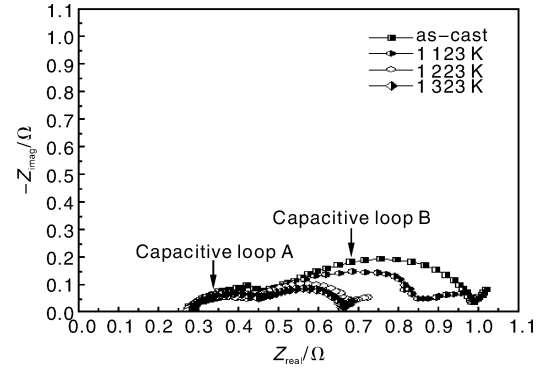
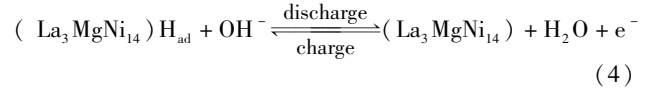


Fig. 6 Electrochemical impedance spectra of the as-cast and annealed alloy electrodes

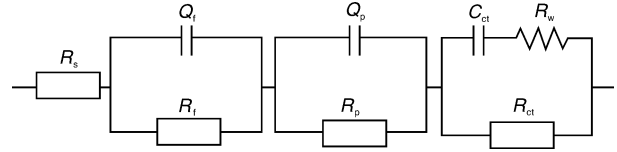


Fig. 7 Proposed equivalent circuit for the alloy electrode

here, in the process of hydrogen releasing reaction, stray capacity and charge-transfer reaction resistance of the electrode are caused by difference of dielectric constant, which is produced by charge-transfer released by LaNi₅ and (La, Mg)₂Ni₇ or (La, Mg)Ni₃ phases of the alloy during hydrogen desorption reaction. It is clearly seen from Table 1 that charge-transfer reaction resistance (R_{ct}) of the alloy electrodes decreases with increasing annealing temperature. Therefore, with increasing annealing temperature, capabilities of hydrogen releasing and number of electrons produced by dehydriding reaction increase in the alloy, and so do electrochemical kinetic characteristics of the alloys, agreeing with HRDs of the alloy electrodes. When frequency is very low, diffusion of hydrogen atom from bulk to surface of the alloy electrode leads to Warburg impedance. Therefore, process of hydrogen desorption of hydride is controlled by electrochemical reaction and hydrogen diffusion.

Table 1 Contact resistance (R_f) and charge-transfer reaction resistance (R_{ct}) of the alloy electrodes

Temperature/K	Contact resistance/mΩ	Charge-transfer reaction resistance/mΩ
as cast	189.9	519.4
1 123	165.5	413.9
1 223	156.9	252.3
1 323	172.6	211.3

4 Conclusions

Effects of annealing treatment on electrochemical properties and structures of La₃MgNi₁₄ alloy electrode are studied in this paper. Annealing treatment has important influence on microstructure of the alloys. As-cast and annealed at 1 123 K alloys

are composed of LaNi_5 , $(\text{La}, \text{Mg})_2\text{Ni}_7$ and a small amount of LaNi_2 phases. Annealing treatment at 1 223 K benefit formation of $(\text{La}, \text{Mg})\text{Ni}_3$ phase. LaNi_5 and $(\text{La}, \text{Mg})\text{Ni}_3$ phases became main phase at 1 323 K. Compared by the as-cast alloy, composition of the annealed alloys is more homogeneous, and grains of the annealed alloys are coarsened after annealing treatment.

With rising annealing temperature, maximum discharge capacity of alloy electrodes increase from $329.1 \text{ mA} \cdot \text{h/g}$ (as-cast) to $383.0 \text{ mA} \cdot \text{h/g}$ (1 323 K). Cyclic life of the alloy electrodes are all improved after being annealed alloys with more homogeneous composition and coarsened grains. Kinetic properties are improved. In three annealed alloys, discharge capacity and cyclic stability of the annealed alloy at 1 323 K has better than that of others in present work.

References

- [1] Ozaki T, Yang H B, Iwaki T, *et al.* Development of Mg-Containing MnNi_5 -Based Alloys for Low-Cost and High-Power Ni-MH Battery[J]. *Journal of Alloys and Compounds*, 2006, 408 - 412; 294 - 300.
- [2] Zhang F L, Luo Y C, Wan D H, *et al.* Structure and Electrochemical Properties of $\text{La}_{2-x}\text{Mg}_x\text{Ni}_{7.0}$ ($x = 0.3 \sim 0.6$) hydrogen storage alloys[J]. *Journal of Alloys and Compounds*, 2007, 439 (1 - 2): 181 - 188.
- [3] Dua Y L, Yang X G, Zhang Q A, *et al.* Phase Structures and Electrochemical Properties of the Laves Phase Hydrogen Storage Alloys $\text{Zr}_{1-x}\text{Ti}_x(\text{Ni}_{0.6}\text{Mn}_{0.3}\text{V}_{0.1}\text{Cr}_{0.05})_2$ [J]. *International Journal of Hydrogen Energy*, 2001, 26(4): 333 - 337.
- [4] Luo J L, Cui N. Effect of Microencapsulation on the Electrode Behavior of Mg_2Ni -Based Hydrogen Storage Alloy in Alkaline Solution[J]. *Journal of Alloys and Compounds*, 1998, 264(1 - 2): 299 - 305.
- [5] Tsukahara M, Kamiya T, Takahashi K, *et al.* *J Electrochem Soc*, 147(2000): 2 941 - 2 944.
- [6] Wang Q D, Chen C P, Lei Y Q. The Recent Research, Development and Industrial Applications of Metal Hydrides in the People's Republic of China[J]. *J Alloys Comp*, 1997, 253 - 254; 629 - 634.
- [7] Zhang X B, Sun D Z, Yin W Y, *et al.* Effect of Mn Content on the Structure and Electrochemical Characteristics of $\text{La}_{0.7}\text{Mg}_{0.3}\text{Ni}_{2.975-x}\text{Co}_{0.525}\text{Mn}_x$ ($x = 0 \sim 0.4$) Hydrogen Storage Alloys[J]. *Electrochimica Acta*, 2005, 50(14): 2 911 - 2 918.
- [8] Kohno T, Yoshida H, Kawashima F, *et al.* Hydrogen Storage Properties of New Ternary System Alloys: La_2MgNi_9 , $\text{La}_3\text{Mg}_2\text{Ni}_{23}$, $\text{La}_3\text{MgNi}_{14}$ [J]. *J Alloys and Comp*, 2000, 311(2): L5 - L7.
- [9] Zhang F L, Luo Y C, Chen J P, *et al.* La-Mg-Ni ternary Hydrogen Storage Alloys with Ce_2Ni_7 -Type and Gd_2Co_7 -Type Structure as Negative Electrodes for Ni/MH batteries[J]. *J Alloys and Comp*, 2007, 430(1 - 2): 302 - 307.
- [10] Pan H G, Liu Y F, Gao M X, *et al.* A Study on the Effect of Annealing Treatment on the Electrochemical Properties of $\text{La}_{0.67}\text{Mg}_{0.33}\text{Ni}_{2.5}\text{Co}_{0.5}$ Alloy electrodes[J]. *Int J Hydrogen Energy*, 2003, 28(1): 113 - 117.
- [11] Pan Y Y, Nash P. *Binary Alloy Phase Diagrams*, Vol. 3[M] // Massalski T B (Ed.). USA OH: ASM International, Metals Park, 1988: 2 406.
- [12] Dunlap B D, Viccaro P J, Shenoy G K. Structural Relationships in Rare Earth-Transition Metal Hydrides[J]. *Journal of the Less Common Metals*, 1980, 74(1): 75 - 79.
- [13] Kohno T, Yoshida, Kanda M. Hydrogen Storage Properties of $\text{La}(\text{Ni}_{0.9}\text{M}_{0.1})_3$ Alloys[J]. *Journal of Alloys and Compounds*, 2004, 363(1 - 2): 254 - 257.
- [14] Hu Mao-pu. *Corrosive Electrochemistry*[M]. Beijing: Metallurgical Industry Press, 1991, 11.
- [15] Kuriyama N, Sakai T, Miyamura H. Electrochemical Impedance and Deterioration Behavior of Metal Hydride Electrodes[J]. *J Alloys and Comp*, 1993, 202(1 - 2): 183 - 197.
- [16] Evgenij B, Macdonald J R. *Impedance Spectroscopy Theory, Experiment and Application*[M]. New Jersey: John Wiley & Sons Incorporation, 2005, 213.

“航空钛合金材料技术现状及发展趋势” 国际研讨会将在京召开

会议地点: 北京·国家会议中心 会议时间: 2011年6月23日

网址: www.ti-2011.com

会议主席: 徐占斌 贺东风 康 义 张彦仲 周 廉

主办单位: 中国航空工业集团公司

中国商用飞机有限责任公司

中国有色金属学会

承办单位: 中国航空工业集团公司基础技术研究院

中国航空工业集团公司北京航空材料研究院

支持单位: 中国工程院 国家发展和改革委员会 美国波音公司

美国通用电气公司 英国罗尔斯-罗伊斯公司